IEEE Photonics Journal
An IEEE Photonics Society Publication

Wavelength-Spacing Switchable Dual-Wavelength Single Longitudinal Mode Thulium-Doped Fiber Laser at 1.9 μm

Volume 8, Number 6, December 2016

Wanzhuo Ma
Tianshu Wang
Yuwei Su
Yan Zhang
Peng Liu
Qingsong Jia
Peng Zhang
Huilin Jiang

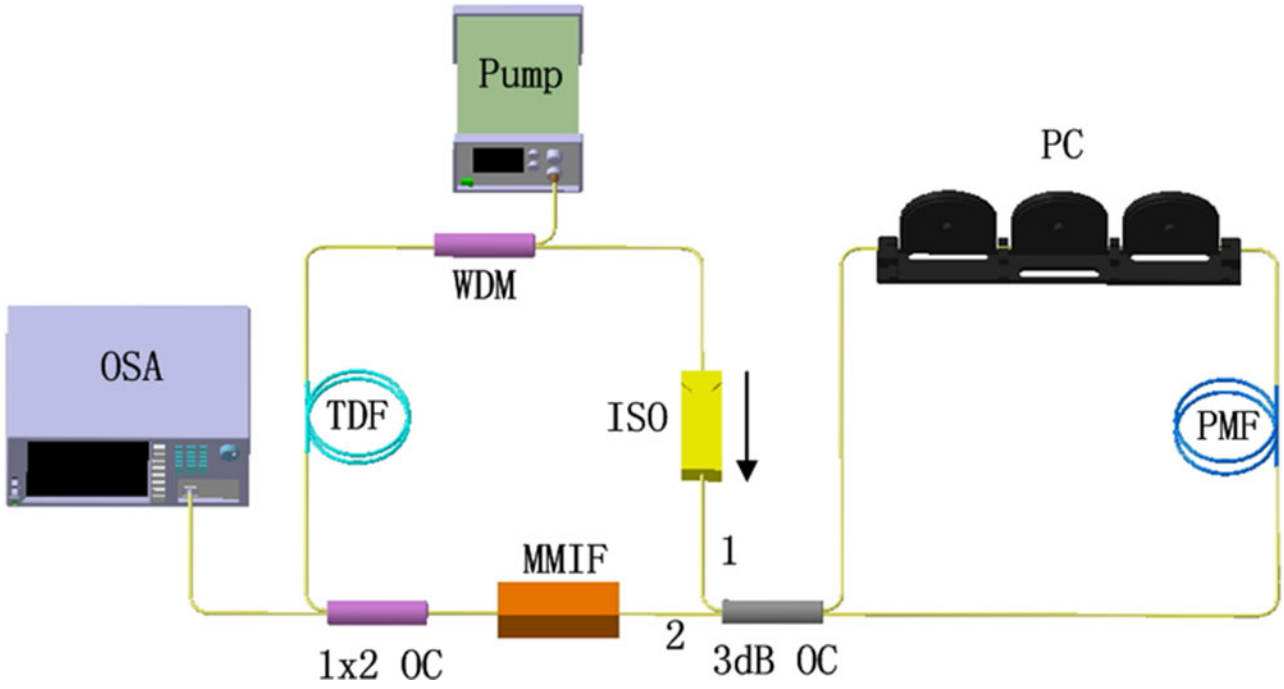

DOI: 10.1109/JPHOT.2016.2616515
1943-0655 © 2016 IEEE

Wavelength-Spacing Switchable Dual-Wavelength Single Longitudinal Mode Thulium-Doped Fiber Laser at 1.9 μm

Wanzhuo Ma,[1] Tianshu Wang,[2] Yuwei Su,[3] Yan Zhang,[3] Peng Liu,[3] Qingsong Jia,[1] Peng Zhang,[2] and Huilin Jiang[2]

[1]College of Opto-Electronic Engineering, Changchun University of Science and Technology, Changchun 130022, China
[2]National and Local Joint Engineering Research Center of Space Optoelectronics Technology, Changchun University of Science and Technology, Changchun 130022, China
[3]College of Science, Changchun University of Science and Technology, Changchun 130022, China

DOI:10.1109/JPHOT.2016.2616515

Manuscript received August 31, 2016; revised September 18, 2016; accepted October 7, 2016. Date of publication October 12, 2016; date of current version November 16, 2016. This work was supported in part by the National Natural Science Foundation of China under Grant 60907020 and in part by the Nature Science Fund of Jilin Province under Grant 20150101044. Corresponding author: T. Wang (e-mail: wangts@cust.edu.cn).

Abstract: We propose and demonstrate a spacing switchable dual-wavelength single longitudinal mode thulium-doped fiber laser at 1.9 μm. The fiber laser employs a ring cavity and a segment of 4-m thulium-doped fiber pumped by a 1563 nm laser. A fiber Sagnac loop is used as a comb filter to generate a stable dual-wavelength laser. A multimode interference filter consisting of a single-mode–multimode–single-mode fiber and a rotary fiber squeezer is used to adjust the wavelength spacing. When pump power is fixed at 260 mW, a stable dual-wavelength laser at 1.9 μm is obtained by adjusting the polarization controller in the Sagnac filter, and the wavelength spacing can be tuned from 6.7 to 26.7 nm by adjusting the rotary fiber squeezer in the multimode interference filter. Each wavelength of the dual-wavelength laser operates at a single longitudinal mode state, and the maximum linewidth is 7.5 MHz analyzed by a Fabry–Perot scanning interferometer.

Index Terms: Fiber laser, dual-wavelength laser, stability, single longitudinal mode.

1. Introduction

The multi-wavelength fiber laser has the advantage of the simple structure and high stability. It can be widely used in the fields of optical communication, fiber sensing and optical measurement, *et al.* Many methods have been adopted to obtain multi-wavelength laser, such as fiber Bragg grating arrays [1]–[3], fiber comb filter [4], [5], stimulated Brillouin scattering [6]–[8], and spatial mode beating effect [9]–[11]. In the most recent reports, there are also some new methods to obtain multi-wavelength lasers, such as the Brillouin-Raman effect [12], random distributed feedback [13], [14], Germania-doped fiber [15], and chalcogenide microwires [16], which have the advantages of wavelength number, narrow linewidth, and mode-locked laser generation.

As an important multi-wavelength laser, the all-fiber dual-wavelength laser has attracted much attention due to its promising application in many optical frontier fields such as microwave photonics,

optical communication, and terahertz wave generation [17]–[19]. The reported researches of the dual-wavelength fiber lasers mainly focused on ytterbium-doped fiber (YDF) laser at 1 μm and erbium-doped fiber (EDF) laser at 1.55 μm band [20]–[23]. The gain region of thulium-doped fiber (TDF) can reach over 300 nm from 1.8 μm to 2.1 μm. Because of the high transmitting loss in silica fiber, stimulated Brillouin scattering and other nonlinear effects are less adopted to generate dual-wavelength fiber laser or compress the linewidth of thulium-doped fiber laser (TDFL). The reported 2 μm tunable dual-wavelength fiber lasers mainly used the spatial mode beating filter and the high-birefringence fiber Bragg grating, but the improvements of these lasers are limited by the instability and the high cost [24], [25]. Thus, tunable dual-wavelength TDFLs have great research value on the tuning range, the stability, the linewidth, and the mode characteristics.

Soltanian *et al*. have reported the dual-wavelength fiber lasers based on photonic crystal fiber, and they show a wide tuning range at 1.5 μm and good stability at 1.9 μm [19], [26]. In our previous works, a multi-wavelength TDFL based on multi-mode interference effect was studied, and the tunable multi-wavelength laser at 2 μm was obtained by using stress on the multi-mode fiber [27]. A widely tunable multi-wavelength laser was also reported based on a modified Mach-Zehnder interferometer and a multi-mode interference filter (MMIF), and the tunable dual-wavelength laser was observed by using a hybrid filter. The experimental results show that the MMIF can be used as an effective tunable wavelength selection device and the hybrid filter can increase the tuning range and the wavelength number [28].

In this paper, we propose and demonstrate a switchable dual-wavelength TDFL. A classic fiber Sagnac loop is used to generate stably dual-wavelength laser at 1.9 μm. A MMIF is used to switch the wavelength spacing of the dual-wavelength laser. Switchable dual-wavelength laser is achieved when pump power fix at 260 mW and the wavelength spacing can be tuned from 6.7 nm to 27.2 nm. The laser modes and the linewidth are measured by a Fabry-Perot interferometer. Experimental results show that each lasing of the dual-wavelength laser operates at a single longitudinal mode state.

2. Experimental Setup and Operation Principle

The configuration of the switchable ring single longitudinal mode dual-wavelength TDFL is shown in Fig. 1(a). A segment of single-mode TDF (NUFERN SM-TSF-9/125) is pumped by a 1563 nm fiber laser with the maximum output power of 500 mW. The numerical aperture, the cut-off wavelength, the mode field diameter, and the lengths of the TDFs are 0.15, 1700 ± 100 nm, 10.5 μm, and 4 m, respectively. A polarization insensitive isolator is used to ensure the laser propagating in a single direction. A fiber Sagnac loop serves as a comb filter to generate stable dual-wavelength laser. A MMIF including a segment of multimode (MM) fiber between two singlemode (SM) fibers (SM-MM-SM) and a rotary fiber squeezer (Thorlabs PLC-900) is used to tune the wavelength-spacing of the dual-wavelength laser as shown in Fig. 1(b). All the fiber components are spliced in a fiber ring cavity by each pigtail. We observed the output spectrum at the 10% port of the 1×2 coupler by an optical spectrum analyzer (OSA, Yokogawa AQ6375) with the resolution of 0.05 nm. The modes and the linewidth of the laser are analyzed by a Fabry-Perot scanning interferometer (Thorlabs, SA-200) with the free spectral range (FSR) of 1.5 GHz from 1250 nm to 2000 nm spectral region.

2.1 Sagnac filter

The fiber Sagnac loop has been widely used as a comb filter to obtain equal-spacing multi-wavelength laser in many previous works. A classical fiber Sagnac loop consists of a 3 dB coupler, a polarization controller (PC), and a segment of polarization maintaining fiber (PMF) as shown in Fig. 1(a). The incident beam launches into port1 of the 3 dB coupler and is divided into two counter-propagating beams with same intensity. The two beams propagate through the PC and the PMF, respectively, and then, they interfered with the 3 dB coupler. The transmission characteristics

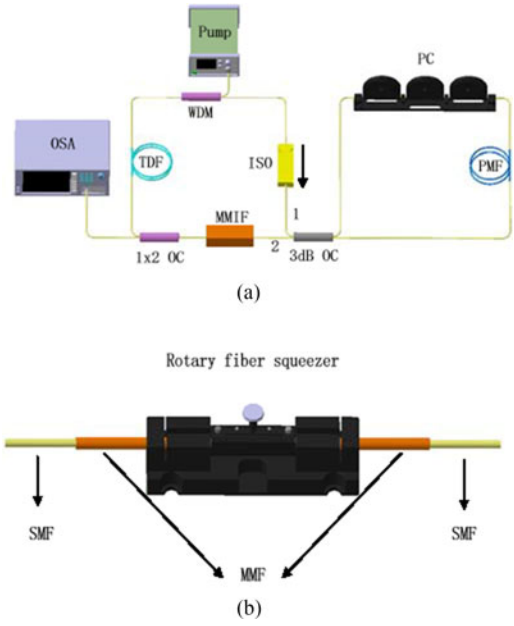

Fig. 1. Experimental setup of the switchable dual-wavelength TDFL.

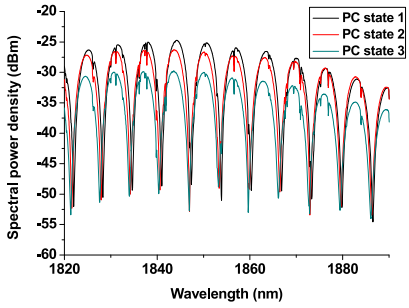

Fig. 2. Transmission spectrum of Sagnac filter.

at port2 can be expressed in

$$T = \sin^2\theta\cos^2\varphi \tag{1}$$

where θ is the polarization deflection angle of the PC. $\varphi = \pi L\,\Delta n/\lambda$ is the phase difference between the fast axis and the slow axis of the PMF, where L is the fiber length of PMF, and Δn is the effective refractive index difference between the two orthogonal axes. We launch a TDF superfluorescent source into port1 of the 3 dB coupler and the transmission spectrum is shown in Fig. 2, and then the Sagnac loop comb filter period of 6.7 nm can be seen and the filtering depth can be changed by adjusting the PC state. Fig. 3 shows the four-wavelength laser at 1.9 μm, the wavelength number can be changed by adjusting the PC due to the changing of the filtering depth. When the laser operates with a stable wavelength number, the mode competition can be mitigated by slightly adjusting the pump power and the PC state. The wavelength spacing corresponds to the period of Sagnac filter, so it can be changed by adjusting the parameters of the PMF given by

$$\Delta\lambda = \lambda^2/L\,\Delta\mathrm{n}. \tag{2}$$

In the experiment, the values of L is 3.1 m. Thus, we can calculate the value of Δn about 1.7×10^{-4}.

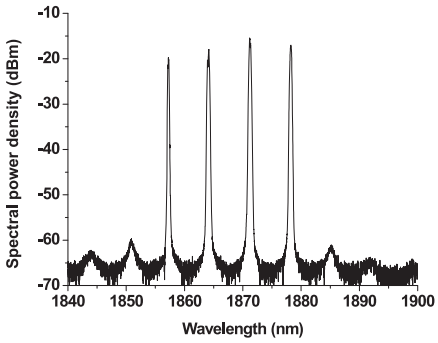

Fig. 3. Four-wavelength laser generated by Sagnac filter.

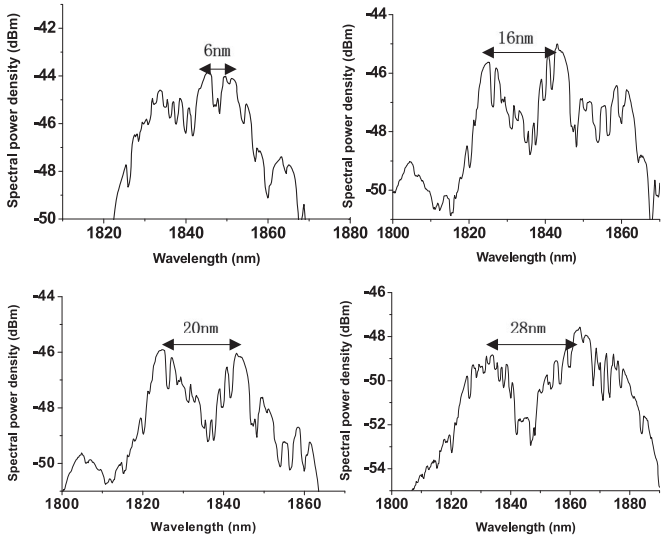

Fig. 4. Transmission spectrum of tunable multimode interference filter.

2.2 Tunable multimode interference filter

In the MMIF, both ends of the multi-mode fiber (MMF) are fusion-spliced with single-mode fiber (SMF). Multiple modes are stimulated when beam propagates from incident SMF to MMF and multi-mode interference effect takes place in the MMF. The interfered peak wavelength of the transmission spectrum at the exiting SMF can be expressed as

$$\lambda = \mathrm{p} \cdot \frac{D_{MMF}^2 n_{MMF}}{L_{MMF}}, \ p = 0, \ 1, \ 2, \ \ldots \tag{3}$$

where D_{MMF}, n_{MMF}, and L_{MMF} are the core diameter, the refractive index and the length of MMF, respectively, and p is positive integer. From (3), one can see that the wavelength spacing of transmission spectrum can be adjusted by choosing different values of D_{MMF} n_{MMF}, and L_{MMF}. In the experiment, we embed the middle segment of MMF into a rotary fiber squeezer as shown in Fig. 1(b) and the effective value of L_{MMF} can be changed when we rotate the fiber squeezer. The core diameter, cladding diameter, and length of MMF are 62.5 μm, 125 μm, and 0.75 m, respectively, and the total insertion loss of the filter is about 3.7 dB. Fig. 4 shows the transmission spectrum of the tunable multimode interference filter. The peak spacing can be tuned from 6 nm to 28 nm due to the change of effective length of MMF by adjusting the fiber squeezer, and the fluctuations of the peak wavelength at each filtering position are all less than 0.7 nm in 30 minutes.

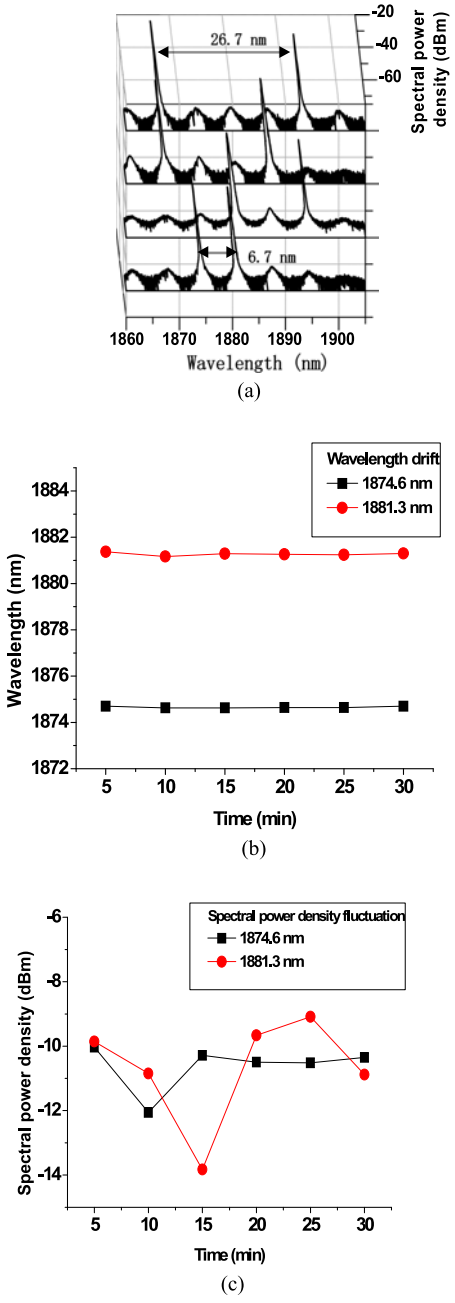

Fig. 5. Dual-wavelength laser with different wavelength spacing and the stability in 30 min.

3. Results and discussions

In the experiment, the self-start is observed when the pump power reaches single-wavelength laser threshold (165 mW), due to the increasing of the filtering effect and the wavelength number with the pump power. From Fig. 2 and Fig. 4, the filtering depth of Sagnac filter is deeper than 15 dB which is obviously better than the filtering depth of the MMIF. Thus the threshold of the multi-wavelength laser is mainly determined by the filtering depth of Sagnac filter. We fix the pump power at 260 mW and stable dual-wavelength laser at 1.9 μm can be obtained by carefully adjusting the PC. By rotating the fiber squeezer to change the spacing of MMIF transmission spectrum, the wavelength

Table 1
Stability measurements of dual-wavelength lasers in 30 min

Wavelength spacing (nm)	Wavelength drift 1 (nm)	Wavelength drift 2 (nm)	Spectral power density fluctuation 1 (dB)	Spectral power density fluctuation 2 (dB)
6.7	±0.035	±0.1	±1.15	±1.869
13.4	±0.04	±0.025	±0.842	±0.47
19.9	±0.015	±0.15	±1.326	±1.92
26.7	±0.1	±0.035	±0.1	±0.712

spacing of the dual-wavelength laser can be switched when the two peaks of MMF transmission spectrum coincide with the Sagnac peaks. The wavelength spacing can be switched from 6.7 nm to 26.7 nm, almost corresponding to the integer times of the Sagnac period, as shown in Fig. 5(a). The side mode suppression ratio (SMSR) decreases from 53 dB to 46 dB when the spacing is tuned from 6.7 nm to 26.7 nm. The decreasing of the SMSR is influenced by the flatness of the amplified spontaneous emission (ASE) spectrum with the peak gain at 1880 nm. Fig. 5(b) and (c) show examples of the wavelength drift and spectral power density fluctuation with 6.7 nm spacing. The wavelength drift is less than ±0.1 nm and the spectral power density fluctuation is less than ±1.869 dB in 30 minutes. During the tuning process, the wavelength drift is always less than ±0.15 nm around the average wavelength and the spectral power density fluctuation is less than ±1.92 dB around the average spectral power density as shown in table 1. The measured stability is better than our previous work which we only used MMIF to obtain multi-wavelength laser at 1.9 μm [27]. The mode competition can be suppressed between the two lasing because the Sagnac fiber loop is a stably wavelength filter with a deep filtering depth and the broad wavelength space. Therefore, the stability of the wavelength and the power are improved. The wavelength drift and the spectral power density fluctuation are mainly caused by the variety of the transmission spectrum of the MMIF which is sensitive to the external stress and the temperature [29], [30]. We can deduce that the stability can be further improved by holding the MMIF in a soundproof box. The wavelength number is determined by the pump power and the polarization state of the PC. The wavelength spacing is determined by the rotary angle of the fiber squeezer. The wavelength number and spacing are unchanged each time the laser is tuned on when the pump power, the polarization state of the PC, and the rotary angle of the fiber squeezer are fixed. Actually, it should be noted that the spacing of dual-wavelength is not continuously adjustable. Dual-wavelength is more easily achieved around the peak of Sagnac period. To shorten the switchable step of the dual-wavelength spacing, the Sagnac period needs to be decreased. Thus a segment of PMF with longer length or higher value of Δn is needed from (2).

We launch the output laser into a Fabry-Perot scanning interferometer and the interfered signal is observed by an oscilloscope with 100 MHz bandwidth as shown in Fig. 6 (a). From Fig. 6 (a), two lines in each free spectral range (FSR) can be seen. Then, we adjust PC to make sure the output laser operating at single-wavelength, one of the interfered lines disappears and there is only one interfered line in each FSR shown in Fig. 6 (b). Fig. 6(c) shows a single line of the interfered signal and the linewidth of dual-wavelength laser can be calculated by

$$\Delta = \frac{t}{T} FSR \tag{4}$$

where t is the full width at half-maximum (FWHM) of the single interfered line (55 μs), and T is the time range of one trigger period (11 ms). The measured linewidth is about 7.5 MHz, which is narrower than the spacing of longitudinal modes (13.6 MHz) of the fiber ring cavity corresponding to the experimental cavity length of 15 m. Thus, we can deduce that each wavelength of dual-

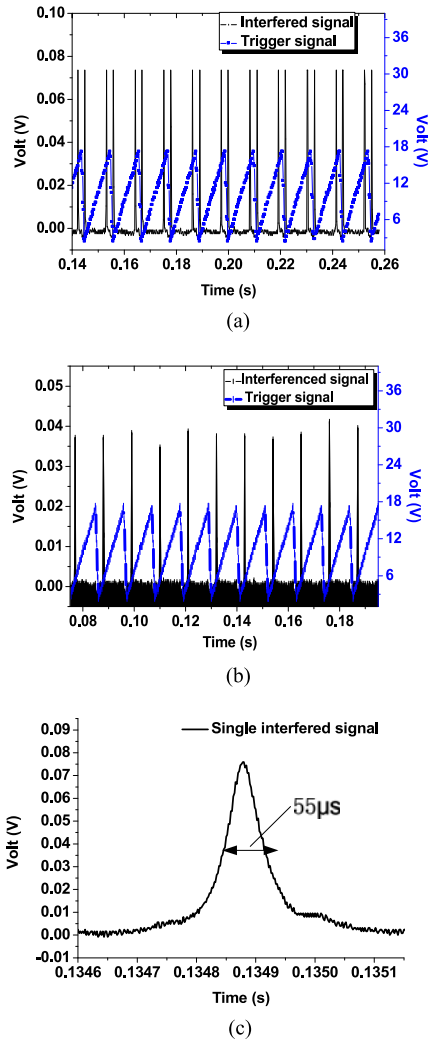

Fig. 6. Interfered signal observed by oscilloscope.

wavelength laser operates at a single longitudinal mode state. It should be noted that the real linewidth should be narrower than the measured linewidth of 7.5 MHz because the resolution of Fabry-Perot scanning interferometer is only 7.5 MHz with the fineness of 200.

4. Conclusion

In conclusion, we have demonstrated a switchable narrow linewidth dual-wavelength TDFL at 1.9 μm. A fiber Sagnac loop is used as a comb filter to generate stably dual-wavelength laser and a MMIF is used to switch the wavelength spacing of dual-wavelength laser. Switchable dual-wavelength laser is achieved when pump power fix at 260 mW and the wavelength spacing can be tuned from 6.7 nm to 26.7 nm corresponding to integer times of the Sagnac period. The wavelength drift is always less than $\pm$0.15 nm and the spectral power density fluctuation is less than $\pm$1.92 dB in 30 minutes. The laser linewidth is measured by a Fabry-Perot scanning interferometer and each lasing of the dual-wavelength laser operates at a single longitudinal mode state. Experimental results show that the hybrid filtering structure has the advantage of large tuning range. The stability can be greatly improved by optimizing the operating environment of the MMIF in subsequent research.

References

[1] Y.-G. Han, F. Fresi, and L. Poti, "Continuously spacing-tunable multiwavelength semiconductor-opticalamplifier-based fiber ring laser incorporating a superimposed chirped fiber Bragg grating," *Opt. Lett.*, vol. 32, no. 9, pp. 1032–1034, 2007.

[2] B. K. Choi, I.-G. Park, and J. H. Byun, " A widely tunable dual-wavelength fiber laser incorporating two polymer waveguide Bragg gratings," *Laser Phys. Lett.*, vol. 10, 2013, Art. no. 125105.

[3] S. R. Rodrigo, L. R. Cobo, and M. A. Quintela, "Dual-wavelength single-longitudinal mode fiber laser using phase-shift Bragg gratings," *IEEE J. Sel. Topics Quantum Electron.*, vol. 20, no. 5, Sep./Oct. 2014, Art. no. 0900305.

[4] T. Wang, X. Miao, X. Zhou, and S. Qian, "Tunable multiwavelength fiber laser based on a double Sagnac Hibi fiber loop," *Appl. Opt.*, vol. 51, no. 10, pp. 111–116, 2012.

[5] A. Luo, Z. Luo, and W. Xu, "Tunable and switchable multiwavelength erbium-doped fiber ring laser based on a modified dual-pass Mach-Zehnder interferometer," *Opt. Lett.*, vol. 34, no. 14, pp. 2135–2137, 2009.

[6] M. H. Al-Mansoori and M. A. Mahdi, "Reduction of gain depletion and saturation on a Brillouin–erbium fiber laser utilizing a Brillouin pump preamplification technique," *Appl. Opt.*, vol. 48, no. 18, pp. 3424–3428, 2009.

[7] G. Mamdoohi, A. R. Sarmani, and A. F. Abas, "20GHz spacing multi-wavelength generation of Brillouin-Raman fiber laser in a hybrid linear cavity," *Opt. Exp.*, vol. 21, no. 16, pp. 18724–18732, 2013.

[8] A. K. Zamzuri, M. H. Al-Mansoori, and N. M. Samsuri, "Contribution of Rayleigh scattering on Brillouin comb line generation in Raman fiber laser," *Appl. Opt.*, vol. 49, no. 18, pp. 3506–3510, 2010.

[9] A. J. Pousite and N. Finlayson, "Multiwavelength fiber laser using a spatial mode beating filter," *Opt. Lett.*, vol, 19, no. 10, pp. 716–718, 1994.

[10] C. Zhao, S. Yang, and H. Meng, "Effcient multi-wavelength fiber laser operating in L-band," *Opt. Commun.*, vol. 204, nos. 1–6, pp. 323–326, 2002.

[11] J. Cheng, L. Zhang, and K. Sharafudeen, "Room-temperature switchable triple-wavelength operation of an erbium-doped fiber laser," *Laser Phys.*, vol. 24, 2014, Art. no. 015102.

[12] X. Li *et al.*, "Improved multiple-wavelength Brillouin-Raman fiber laser assisted by four-wave mixing with a micro-air cavity," *Appl. Opt.*, vol. 54, no. 33, pp. 9919–9924, 2015.

[13] M. Bravo, V. D. Miguel, A. Ortigosa, and M. Lopez-Amo, "Fully-switchable multi-wavelength fiber lasers based on random distributed feed-back for sensors interrogation," *J. Lightw. Technol.*, vol. 33, no. 12, pp. 2598–2605, Jun. 2015.

[14] D. Leandro, S. Rotarodrigo, D. Ardanaz, and M. Lopez-Amo, "Narrow-linewidth multi-wavelength random distributed feedback laser," *J. Lightw. Technol.*, vol. 33, no. 17, pp. 3591–3696, Sep. 2015.

[15] T. Huang *et al.*, "All-fiber multiwavelength thulium-doped laser assisted by four-wave mixing in highly Germania-doped fiber," *Opt. Exp.*, vol. 23, no. 1, pp. 340–348, 2015.

[16] A. A. Kadry, M. E. Amraoui, Y. Messaddeq, and M. Rochette, "Mode-locked fiber laser based on chalcogenide mi-crowires," *Opt. Lett.*, vol. 40, no. 18, pp. 4309–4312, 2015.

[17] S. Mo *et al.*, "Microwave signal generation from a dual-wavelength single-frequency highly Er^{3+}/Yb^{3+} Co-doped phosphate fiber laser," *IEEE Photon. J.*, vol. 5, no. 6, Dec. 2013, Art. no. 5502306.

[18] R. K. Kim, S. Chu, and Y. G. Han, "Stable and Widely tunable single-longitudinal-mode dual-wavelength Erbium-Doped fiber laser for optical beat frequency generation," *IEEE Photon. Technol. Lett*, vol. 24, no. 6, pp. 521–523, Mar. 2012.

[19] M. R. K. Soltanian, I. S. Amiri, S. E. Alavi, and H. Ahmad, "Dual-wavelength erbium-doped fiber laser to generate terahertz radiation using photonic crystal fiber," *J. Lightw. Technol.*, vol. 33, no. 24, pp. 5038–5046, Dec. 2015.

[20] A. R. EL-Damak, J. Chang, J. Sun, C. Xu, and X. Gu, "Dual-wavelength, linearly polarized all-fiber laser with high extinction ratio," *IEEE Photon. J.*, vol. 5, no. 4, 2013, Art. no. 1501406.

[21] H. Ahmad, M. R. K. Soltanian, C. H. Pua, M. Z. Zulfil, and S. W. Harun, "Narrow spacing dual-wavelength fiber laser based on polarization dependent loss control," *IEEE Photon. J.*, vol. 5, no. 6, 2013, Art. no. 1502706.

[22] M. I. Md Ali *et al.*, "Tapered-EDF-based mach–zehnder interferometer for dual-wavelength fiber laser," *IEEE Photon. J.*, vol. 6, no. 5, Oct. 2014, Art. no. 5501209.

[23] B. Yin, S. C. Feng, Z. B. Liu, Y. Bai, and S. Jian, "Tunable and switchable dual-wavelength single polarization narrow linewidth SLM erbiumdoped fiber laser based on a PM-CMFBG filter," *Opt. Exp.*, vol. 22, no. 19, pp. 22528–22533, 2014.

[24] S. Wang, P. Lu, S. Zhao, D. Liu, W. Yang, and J. Zhang, "2- μm switchable dual-wavelength fiber laser with cascaded filter structure based on dual-channel Mach–Zehnder interferometer and spatial mode beating effect," *Appl. Phys. B*, vol. 117, no. 2, pp. 563–569, 2014.

[25] W. J. Peng *et al.*, "1.94 μm switchable dual-wavelength Tm3+ fiber laser employing high-birefringence fiber Bragg grating," *Appl. Opt.*, vol. 52, no. 19, pp. 4601–4607, 2013.

[26] M. R. K. Soltanian, H. Ahmad, A. Khodaie, I. S. Amiri, M. F. Ismail, and S. W. Harun, "A stable dual-wavelength Thulium-doped fiber laser at 1.9 μm using photonic crystal fiber," *Sci. Rep.*, vol. 5, 2015, Art. no. 14537.

[27] P. Zhang, T. S. Wang, W. Z. Ma, K. Dong, and H. Jiang, "Tunable multiwavelength Tm-doped fiber laser based on the multimode interference effect," *Appl. Opt.*, vol. 54, no. 15, pp. 4667–4671, 2015.

[28] W. Z. Ma, T. S. Wang, P. Zhang, J. Han, and J. Zhang, "Widely tunable multiwavelength thulium-doped fiber laser using a fiber interferometer and a tunable spatial mode-beating filter," *Appl. Opt.*, vol. 54, no. 12, pp. 3786–3791, 2015.

[29] E. Li, "Temperature compensation of multimode-interference-based fiber devices," *Opt. Lett.*, vol. 32, no. 14, pp. 2064–2066, 2007.

[30] A. M. Hatta, Y. Semenova, Q. Wu, and G. Farell, "Strain sensor based on a pair of single-mode-multimode-single-mode fiber structures in a ratiometric power measurement scheme," *Appl. Opt.*, vol. 49, no. 3, pp. 536–541, 2010.